Power load characterization for Type-I ELMy H-Modes in JET

H.Thomsen[1], T.Eich[1], S.Devaux[1], G.Arnoux[2], S.Brezinsek[3], E.delaLuna[4,5], W.Fundamenski[2], A.Herrmann[1], A.Huber[3], S.Jachmich[4,6], P.Lomas[2], I.Nunes[4,7], G.Saibene[8], A.Scarabosio[1], J.Schweinzer[1] and JET EFDA Contributors[*]

JET-EFDA, Culham Science Centre, Abingdon, OX14 3DB, UK
1) Max-Planck-Institut für Plasmaphysik, EURATOM-Association, D-17491 Greifswald, Germany
2) Culham Science Centre, EURATOM/CCFE Fusion Association, Abingdon, OX14 3DB, UK
3) IPP-Energieforschung, Forschungszentrum Jülich GmbH, Association EURATOM, 52425 Jülich, Germany
4) EFDA-CSU, Culham Science Centre, Abingdon, OX14 3DB, UK
5) Laboratorio Nacional de Fusión, Asociación EURATOM-CIEMAT, Madrid, Spain
6) ERM/KMS, Association EURATOM - 30 Avenue de la Renaissance B-1000 Brussels, Belgium
7) Associação EURATOM-IST, Instituto de Plasmas e Fusão Nuclear – L.A., IST, Lisboa, Portugal
8) Fusion for Energy Joint Undertaking, 08019, Barcelona, Spain

E-mail contact of main author: henning.thomsen@ipp.mpg.de

Abstract. Following the installation of a fast high resolution infrared (IR) system viewing the JET divertor and using the existing wide-angle IR-camera a large number of experiments have been performed optimized for power exhaust studies with focus on ELM and inter-ELM profiles. Type-I ELMy H-mode deuterium plasmas with currents from 1MA-3.8MA, q_{95}=3.3-5.4 with low and high triangularity were investigated. The IR camera was validated against divertor thermo-couples, pyrometer signals and Langmuir probes. In the data base an increase of the wetted area with ELM power was observed (corresponding outer mid plane integral power width ranging between 7 mm and 18 mm), but additional scaling parameters explaining the large scatter are not revealed. The ELM temporal shape is characterized. It is found that in the rise phase of the ELM target power the number of these striations increases from 3-5 to numbers around 10-20. In a series of pulses with a varied plasma- wall distance, the ELM mid plane far-SOL radial power decay length is found to be ~23 mm.

1. Introduction

One critical factor in the standard H-mode scenario of the ITER operation is the maximum allowable energy density for transient events on the plasma facing components. The impact of edge localized modes (ELMs) onto the divertor target plates should stay below an energy density of 0.5 MJ/m² per ELM (pulse duration ~500 µs) to avoid a significant reduction of the divertor life time due to material eroision [1]. If the predominant deposited ELM energy density were a factor of 2-3 above this limit, a CFC erosion rate of approximately 1 µm/ELM and large scale melting of W with possible ejection of droplets would occur and could require a replacement of the divertor targets after only ~10000 ELMs.

The expected ELM size in ITER is extrapolated from current day devices based on the multi-machine ν^* scaling [2]. The ELM dynamics in the SOL plays an important role for the spatial and temporal characteristics of the ELMs arriving at the divertor and first wall materials.

Following the installation of a fast high resolution infrared (IR) system viewing at the JET divertor and using the existing wide-angle IR-camera a large number of experiments have been performed optimized for power exhaust studies with focus on ELM and inter-ELM

---

[*] See the Appendix of F. Romanelli et al., paper OV/1-3, this conference

profiles. Type-I ELMy H-Mode deuterium plasmas with currents from 1MA-3.8MA, q_{95} in the range of 3.3-5.4 with low (δ=0.25) and high magnetic configuration triangularity (δ=0.4) were investigated.
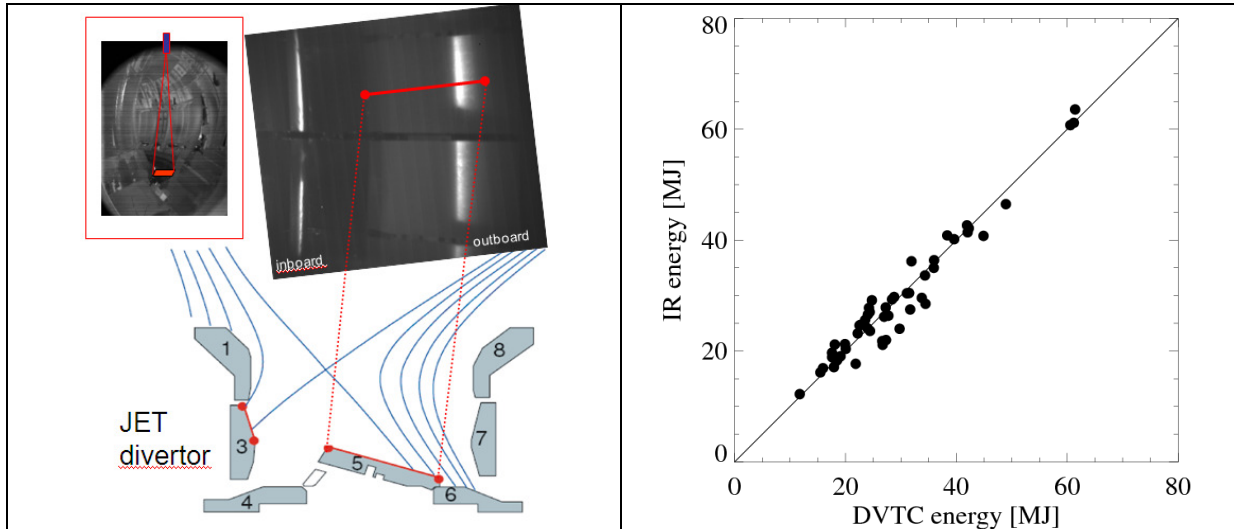
2. Setup, Validation and Methods

FIG 1: (a) Setup of the newly installed IR camera in the JET tokamak. (b) Comparison of IR and thermocouple (DVTC) estimated total energies for 52 discharges in the data base.

The time resolution of the new IR camera installed in the 2008 campaign (FLIR/Titanium, 3-5µm wave length, typical time resolution Δt_{IR}=86 µs, typical stare time 40 µs) allows for ELM resolved measurements of power loads on the JET outboard divertor target (tile 5 in Fig. 1(a)) with a 1.7 mm spatial resolution.

Optical restrictions in the set-up lead to an unfavourable coverage of the inboard target under a sharp angle, leading to a resolution of 5 mm at the inboard target. Especially during ELM times an unknown fraction of the deposited power spills over to the further inboard divertor tile with unknown surface layer properties. In this paper we therefore constrain ourselves to data from the outboard divertor.

The IR based absolute estimate of the surface temperature of the CFC-tiles is validated by comparing with tile embedded divertor thermocouple (DVTC). The discharge integrated energy balance from IR with respect to DVTC is found to lie within a range of 80-120% as shown in Fig. 1(b). Pyrometer temperature measurements at the same divertor tile are available for some discharges and the agreement with the temperature of the IR camera is better than 3 %. Comparison to divertor Langmuir probe measurements (LP) for selected discharges are used to assess the influence of the divertor target surface thermal properties on the inferred heat fluxes by IR for short events such as ELMs [3]. A detailed comparison between IR and LP measurements for a single ELM event with striations resolved by both diagnostics showed an inter-diagnostics time difference in the range of the sampling rate of both diagnostics [4].

The non-linear finite-element code THEODOR code was used to calculate the heat fluxes assuming a 2d geometry and temperature dependent material parameters [5, 6].

The data is divided into ELM and inter-ELM phases and the power on the divertor target as well as the wetted area are estimated for each ELM and inter-ELM phase (~1 ms before the next ELM). The rise time τ_r from the ELM start (steep increase of heat flux) to ELM peak and

the decay time τ_d from ELM peak to 1/e decay are estimated for each individual ELM (cf. Fig 2).
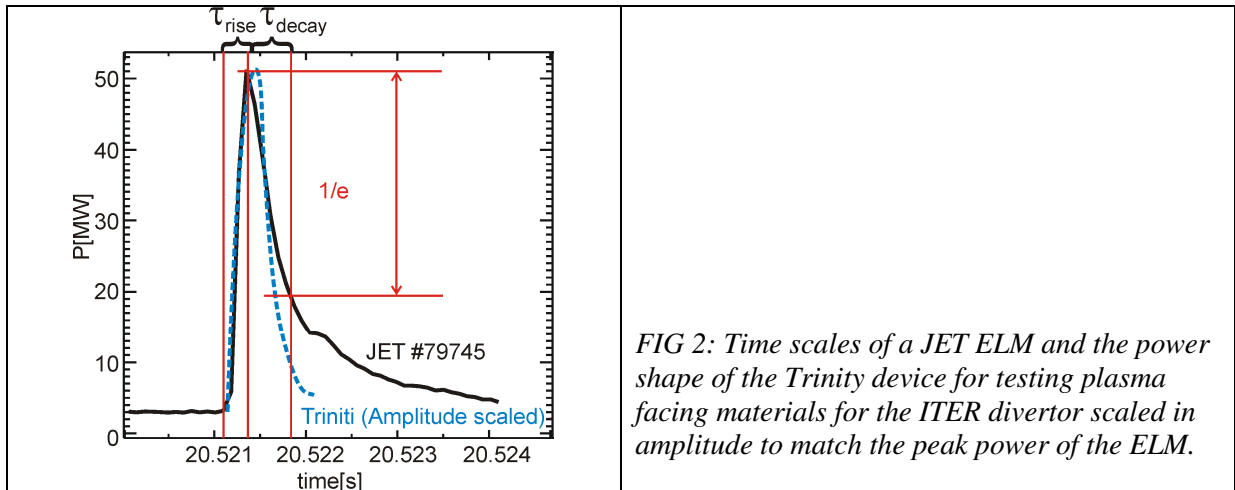
The heat flux profiles for ELM and inter-ELM phases are of special interest in terms of the plasma surface interaction and there are several methods used in the Literature in order to estimate the spatial decay width in the SOL-region from IR target data [7]. Here, we use the wetted area, which can be mapped into an integral deposited power width considering the magnetic flux expansion from the target to the outer mid plane. The wetted area (in m²) is estimated from the ratio between the target-integrated power P (W) and the peak heat flux Q_{peak} (in W/m²), $A_{wet}=P/Q_{peak}$ (m²).

(Peak) ELM energy densities, $\varepsilon= \int Q (s_{peak},t) dt$, with s the spatial coordinate, are calculated for a poloidal average of 1 cm centered around the position s_{peak} of the ELM peak location. The integration time is from the ELM start (steep increase of heat flux) until the 1/e decay after the ELM peak. Note, that this definition of ε characterizes the local peak energy density in contrast to an integral definition via the ratio between target deposited energy and wetted area. In terms of material erosion limits by power transients, the peak energy density should be more relevant since the erosion will occur localized as well.

For the ELM wetted area a second approach can be utilized, the ratio between the energy (J) and the energy density (in J/m²). Since time integrated signals are considered, the latter method should be less affected by an over-estimation of the peak heat flux due to surface layer effects. In fact we find that the second method based on the energy density yields slightly larger values of the wetted area. We show here the (smaller) wetted area estimates based on the first method ($A_{wet}=P/Q_{peak}$), therefore, the wetted area estimates should be conservative.

To characterize the ELM size we use the energy difference ΔW_{MHD} in the plasma stored energy before the ELM and 4 ms after the drop. The relative ELM size is given by normalization to W_{MHD}.

The current data base contains a total of 65 time-windows in 52 discharges, time window intervals ranging from 0.5 s to 12 s. More than 6400 individual ELMs and preceding inter-ELM values are included.
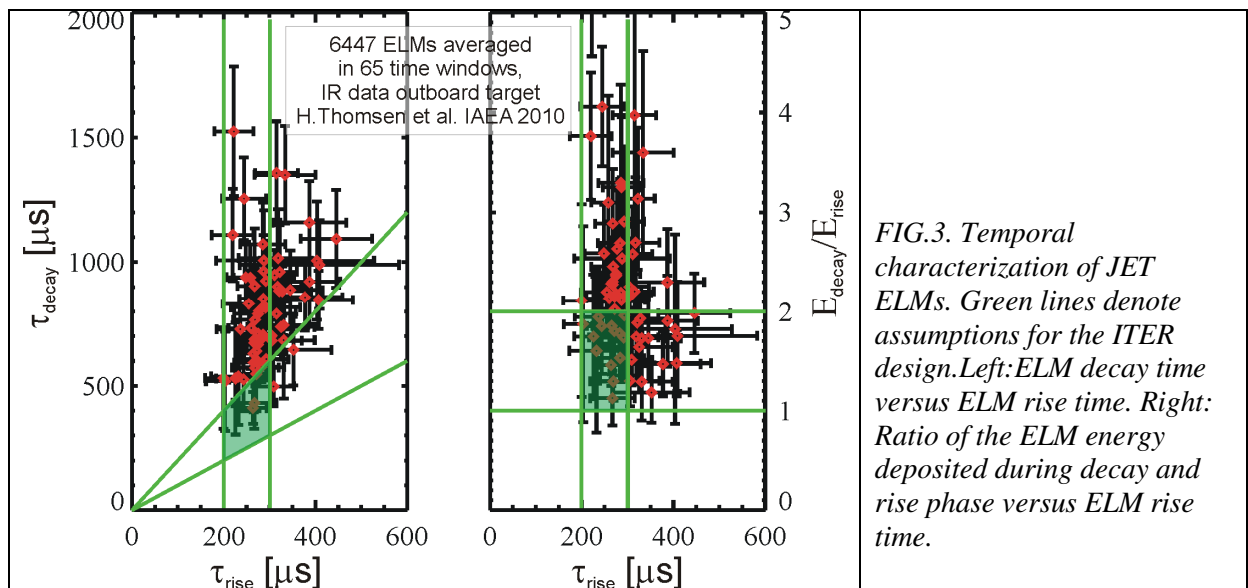

FIG 2: Time scales of a JET ELM and the power shape of the Trinity device for testing plasma facing materials for the ITER divertor scaled in amplitude to match the peak power of the ELM.

3. Temporal characterization of ELM shapes

The time period in which an ELM deposits its power on the divertor target is an important parameter for the estimation of a material limit. The energy density limit currently forseen for the ITER divertor targets is 0.5MJ/m² for ELM pulses with 0.5 ms duration [8,9]. Since also the actual temporal shape of the ELM has an effect on the allowable energy density limit, we

characterize the ELM shape by a rise and a decay time, c.f. Fig. 2. Since the ELM rise time scales with the convective parallel time $\tau_{\parallel}$ ($\tau_{\parallel}=L_c/c_s$, with L_c: connection length, c_s: ion sound speed in the SOL) [2, 10, 11], the absolute time scales for JET and ITER are expected to be nearly identical. For JET a connection length of $L_c=64$ m and a pedestal temperature of $T_{ped}=1$keV results in a $\tau_{\parallel}\sim210$ µs, for ITER the expected pedestal temperature of $T_{ped}=4$ keV and $L_c=120$ m give $\tau_{\parallel}\sim200$ µs. In Fig. 2, the ITER reference ELM power shape of the Triniti divertor material test facility is plotted with a measured JET-ELM power evolution. The rise time of $\tau_r=250$ µs is very similar, the decay time is a little longer for the JET ELM. In Fig. 3 the rise and decay times of a total of 6447 ELMs as measured by the IR camera for a variety of discharge conditions are plotted. The ELMs within a time window (in total 65 time windows) are represented by a data point and an uncertainty interval calculated from the standard deviation of the ELM times within the respective time window. The observed rise times are in the range between 200 µs and 500 µs. The decay times are typically 1.5 to 5 times longer than the corresponding rise times.

The assumptions for ITER ELMs (rise time $\tau_{r,ITER}\sim250$ µs and decay time $\tau_{d,ITER}=250$-500 µs) are therefore conservative, but the observed decay time distribution in JET ELMs is significantly larger than the ITER assumption, $\tau_d > \tau_{d,ITER}$. The ratio of the ELM deposited energy in the rise and decay phase shows a variation from 1 to 5, thus more energy is deposited in the decay phase (for the ITER design a ratio between 1 and 2 is assumed).

FIG.3. Temporal characterization of JET ELMs. Green lines denote assumptions for the ITER design. Left: ELM decay time versus ELM rise time. Right: Ratio of the ELM energy deposited during decay and rise phase versus ELM rise time.

4. Short time ELM physics and filaments

The associated mode numbers of the ELM instability are derived from the distribution of the single divertor target heat load imprints caused by ELM filaments. Their evolution is analysed over the duration of each single ELM (~1-2ms). It is found that in the rise phase of the ELM target power the number of these striations increases from 3-5 to numbers around 10-20 (cf. Fig. 4). The striation number seems to be independent of the input power. A slight dependency on the safety factor q_{95} is possible [12]. A detailed investigation reveals that the increase of the ELM target heat load in an early stage of up to 0.4 τ_r is associated with an increase of the number of single filaments. For later times (>0.4 τ_r) the number of observed striations remains constant and the target heat flux changes according to the power changes of individual striations.
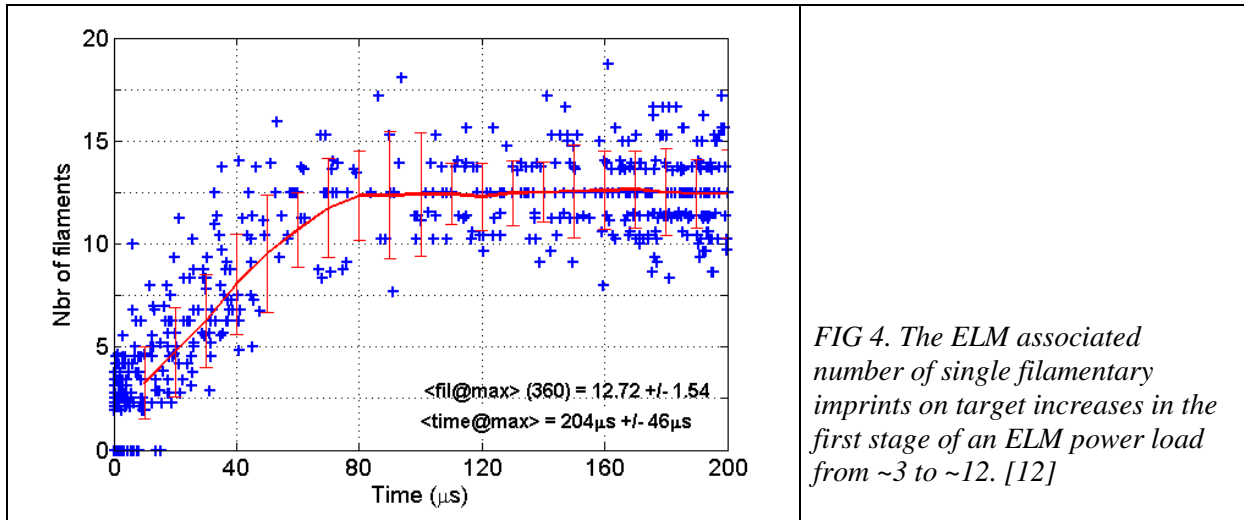
FIG 4. The ELM associated number of single filamentary imprints on target increases in the first stage of an ELM power load from ~3 to ~12. [12]

5. ELM resolved power load scaling

In Fig. 5 the wetted area for ELM peak and inter-ELM times are plotted. For the ELM wetted area, the data in each of the 60 time windows is grouped into energy bands of 1% relative ELM size and the mean as well as the standard deviation is calculated for each of these groups. This way, the ELM wetted area can be calculated for a larger variety of ELM sizes within one time window without losing the ELM size as a parameter. 5 discharges had to be excluded from the data base, since the target surface had a layer very close to the strike-line.

The magnitude of the ELM energy loss was found to order the ELM wetted area in a series of discharges with a scan in TF-ripple [13] and in IR measurements in a D-III-D discharge with a plasma current sweep [14]. This tendency can also be observed in the larger data set presented here: the minimum ELM wetted area increases with the ELM size. In the data base we find wetted areas between 0.6 m² and 1.6 m², corresponding to mid plane integral deposited power widths of 7 mm and 18 mm, respectively.

As yet, no other clear scaling parameter could be identified. The coloured lines are fits to the data grouped by plasma current ranges. The increase of the ELM wetted area with ELM size is observed for all these plasma current groups. However, the scatter inside these groups is rather large and the fits show no obvious ordering with plasma current. We note, that the fitted slopes increase with plasma current. Similar analysis was performed for a grouping in q_{95} bands, but also here the ELM wetted area shows no clearer dependence.

For the inter-ELM wetted area, shown in Fig. 5 as dots, we find a slight decrease with increasing ELM size. The increase in scatter and inter-ELM wetted area in phases with small relative ELM sizes < 2 % is presumably caused by an increasing amount of ELM compound phases mistakenly considered as inter-ELM profiles by the automated analysis software. The average inter-ELM wetted area varies from 0.2 m² to 0.5 m². These areas translate into mid plane integral power widths of 2.5 mm to 6 mm.

The power broadening varies between 1 (ELM wetted area equal to the inter-ELM wetted area) and 5. The target wetted area is found to show a relatively large broadening in the presence of large ELMs and a moderate broadening in conditions with smaller ELMs as shown in Fig. 5.

In Fig. 6 (a) the energy density versus the ELM size is shown. The minimum observed energy density is found to increase with ELM size. The energy density displays a large scatter, which might partly be caused by the uncertainty of the ELM decay time estimation in the presence of compound ELM phases after the main ELM. Some of the largest energy densities in the data set (denoted by coloured squares) are found in three discharges, which are analysed in

more detail in the following. These discharges form a gas fueling scan, where the gas fueling rate was increased from $G=2\cdot10^{22}$ el$\cdot$s^{-1} to $G=4\cdot10^{22}$ el$\cdot$s^{-1} on a shot-by-shot basis. The wetted area and the peak heat flux are shown in Fig. 6 (b,c) for these 3 discharges.
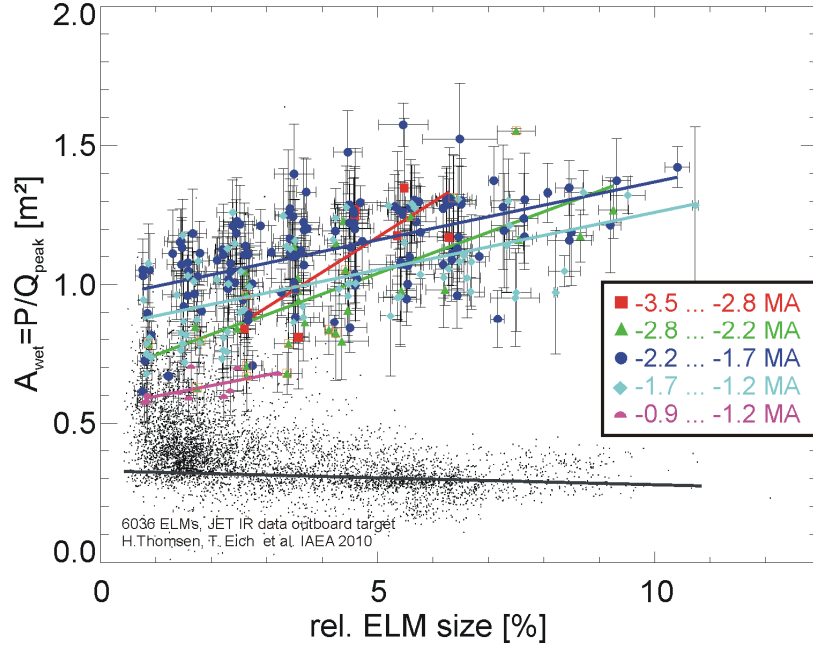

FIG 5: Database of wetted area versus the ELM size normalized to W_{MHD}. Different colours indicate plasma current intervals and solid lines denote linear fits to the wetted area in the respective interval.
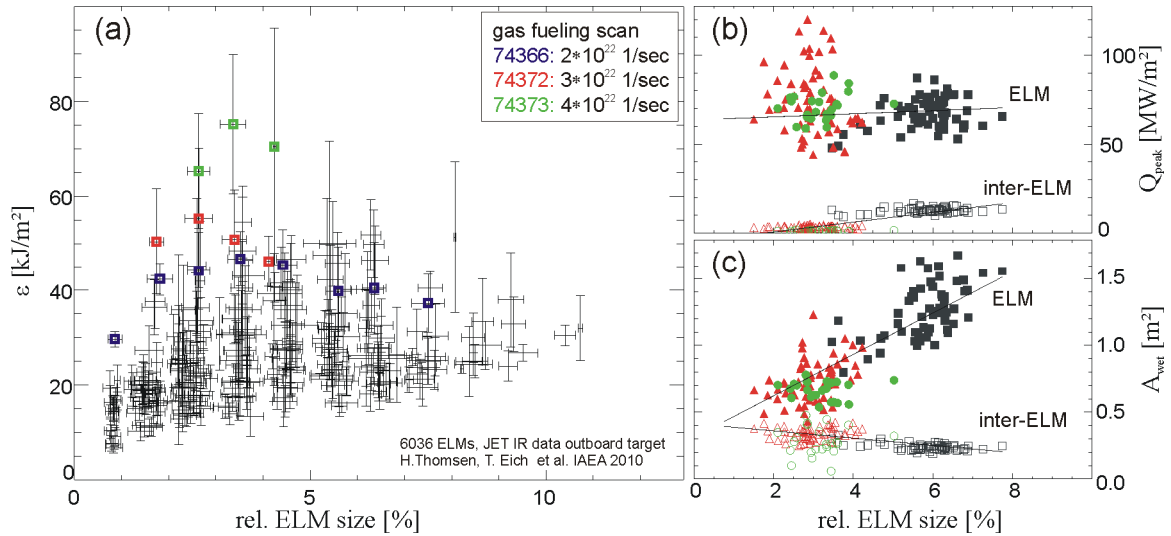

FIG 6: (a) Energy density versus ELM size normalized to W_{MHD} for the data base. Colours denote values from a gas fueling scan. (b) Corresponding peak heat fluxes and (c) wetted areas. Solid lines are linear fits to the data.

The ELM peak power increases roughly linearly with the ELM size (not shown), as does the ELM wetted area (cf. Fig. 6 (c)), but the ELM peak heat flux stays constant (Fig. 6(b)), and some ELMs at the intermediate gas fueling rate (#74372) show an even higher peak heat flux for a reduced ELM size with respect to the reference (#74366). Thus, for these 3 discharges, the increase in the wetted area is caused by the increase in deposited ELM power, only. The

inter-ELM wetted area is decreasing from A=0.35m² at ~2% ELM size to A=0.2 m² at 7% ELM size.

6. ELM heat load impact on the first wall

The impact of ELMs (filaments) on the first wall has been studied by varying the distance of the separatrix to the outer wall limiter from 7.0 cm – 5.2 cm – 4.2 cm on a shot-to-shot basis. These scans were performed separately for different ELM sizes of about 4% and 9% energy loss normalized to the plasma stored energy achieved with mid plane gas puffing for a fixed plasma current of 2.0 MA and toroidal magnetic field of 2.0 T. The ELM mid plane far-SOL radial power decay length is found to be about 23 mm. It is observed that larger ELMs (rel. ELM size ~9%) deposit a larger fraction of their energy onto the limiters than smaller ELMs (~4%). The near SOL ELM power decay length estimated from the target wetted area is 15 mm.

7. Discussion

The relative ELM size estimated from the W_{MHD}-signal apparently orders the data estimated from the IR measurements, like the increase of the wetted are with the ELM size, rather well. An ELM resolved power balance, taking into account the radiated power loss estimated by bolometry, the drop in stored energy and the energy by the total input power on a time scale of 4 ms (constrained by the time resolution of the bolometer system) reveals that the scatter of ΔW_{MHD} is approximately twice as large as the scatter of energy measured at the target. Apart from the different magnitude in ELM size, the general findings (i.e., ELM broadening) are similar for an energy loss estimate 500 µs after the drop instead of 4 ms.

The scatter in the data might partly be associated with the applied semi-automated ELM detection, since the algorithm will also account for ELMs in compound phases. The advantage of this approach is a less biased study of ELM power loads compared to data bases with a small amount of hand-selected ELMs, which would hardly be feasible for the amount of data to be analyzed.

The results on ELM time scales prove the assumptions on ELM time scales in ITER to be conservative, since the observed rise times are as expected also for ITER. It remains to be confirmed in material test facility experiments, that a different temporal evolution of the ELM power load with more energy in the tail is compatible with the adopted energy density limit of 0.5 MJ/m² in 500 µs for transients.

The observed inter-ELM integral deposited power widths as narrow as 2.5 mm are compatible with previously reported values measured by other diagnostics [11]. Results reported from Langmuir probe measurements in JET indicated an ELM broadening [15] although it could not be confirmed by the old IR camera system, presumably due to the limited spatial and temporal resolution. With the new IR system, the broadening can be confirmed to exist and is found to be in the range between 1 and 5, depending on plasma conditions. At this stage, no clear scaling could be identified for the presented JET IR data base, but a multi-variable regression analysis is yet to be performed. Also, since the pedestal data is not yet included in our data base for a larger number of time windows, the normalization to pedestal values and scaling with pedestal parameters remains a task for the future.

The observation in JET and in D-III-D that the power broadening scales with the ELM size is an indication, that such behaviour might also be expected for ITER (more data from other fusion devices and a multi-machine scaling are necessary for gaining confidence in such extrapolation). If this assumption was valid, larger ELMs might be tolerable due to the increased wetted area. A caveat might be the finding that mitigated ELMs reduced in size by

means of gas puffing, may have a larger (peak) energy density than the natural ELMs. With the increase of the ELM frequency observed for mitigation by gas fueling, the smaller ELMs might actually pose a larger threat in terms of target erosion due to their smaller wetted area than larger unmitigated ELM with a large deposition area. However, it is not clear, whether it is possible to establish a stable scenario with large ELMs and a large wetted area. Moreover, the less protected first wall materials outside the divertor target might also get a larger share of the energy due to the enhanced radial transport and the inter-ELM wetted area shows a tendency to decrease as well.

In the case of a small ELM scenario it could be feasible to spread the power load by sweeping the strike lines and thereby effectively wetting a larger divertor target area. The evaluation of ELM mitigation scenarios should therefore include an assessment of the wetted area [16,17].

8. Conclusions

Following the installation of a fast infrared camera at the JET tokamak with a high spatial and temporal resolution allowing for ELM-resolved power load studies, a data base with analyzed IR discharges has been set up. The IR data is validated by means of discharge integrated divertor thermo-couple measurements and to Langmuir probe data.

ELM power broadening is observed to widen with increasing ELM size for a variety of discharge conditions. Furthermore, the ELM shape could be characterized. The ELM rise times are found to be in the expected range, but the deposited energy during the ELM decay is larger than assumed for the ITER design. Further input from other machines is required for a multi-machine scaling necessary for a solid extrapolation to ITER.

Acknowledgements

References

[1] A. Loarte, et al., this conference.
 [2] A. Loarte et al., Plasma Phys. Control. Fusion **45** (2003) 1549.
 [3] S. Jachmich et al., ECA Vol.**33E** (2009) P-2.159.
 [4] T. Eich et al., submitted to J. Nucl. Mater. (2010).
 [5] A.Herrmann et al., J. Nucl.Materials, **337-339** (2005) 907.
 [6] A. Herrmann, Phys. Scr. **T128** (2007) 234.
 [7] A. Loarte et al., J. Nucl.Materials **266-269** (1999) 587.
 [8] J. Linke et al., J. Nucl. Mater. **367-370** (2007) 1422.
 [9] N. Klimov et al., J. Nucl. Materials **390–391** (2009) 721.
[10] T. Eich et al., Plasma Phys. Contr. Fusion **47** (2005) 815.
[11] W. Fundamenski et al., Nucl. Fusion **45** (2005) 950.
[12] S. Devaux et al., submitted to J. Nucl. Mater. (2010).
[13] H. Thomsen et al., ECA Vol.**33E** (2009) P-2.164.
[14] M. Jakubowski et al., Nucl. Fusion **49** (2009) 095013.
[15] S. Jachmich et al., J. Nucl. Mater. **363-365** (2007) 1050.
[16] S. Jachmich et al., submitted to J. Nucl. Mater. (2010).
[17] E. de la Luna et al., this conference.